INTERNAL DOCUMENT

No. 183

POL ABS CALIBRATIONS 2005-2007

B.D. Moate,
P.D.Thorne,
R.D.Cooke and
K.F.E. Betteridge

July 2007

Proudman Oceanographic Laboratory
NATURAL ENVIRONMENT RESEARCH COUNCIL

www.pol.ac.uk

Contents

1 Introduction

Suspended inorganic particles (such as sands) strongly scatter incident acoustic pressure waves at MHz frequencies, with the amplitude of the backscattered pressure being related to the mass concentration and nominal size of the particles in suspension. Over the past two decades, this physical premise has led to the development of transducer based Acoustic Backscatter Systems (ABS), usually designed to collect profile measurements at centimetric resolution over a metre or so of the near-bed region when implemented in sediment transport studies (Thorne and Hanes, 2002). Modern ABSs typically operate (simultaneously) at multiple frequencies, to enable derivation of the nominal particle radius (a_0) from ratios of the backscattering form function at the different frequencies (Thorne and Hardcastle, 1997). The backscattering form function represents the backscattering characteristics of a given particle relative to its geometrical size, and is often expressed in terms of a parameter, x, where $x = 2\pi a_0/\lambda$ (Thorne and Meral, 2007), with λ the acoustic wavelength in water.

In order to relate backscatter data derived from an ABS to particle concentration and size, the ABS requires calibration to determine the system constant at each of its measuring frequencies. An ABS system constant represents the electronic response of the ABS, its transmit and receive sensitivity, and the beam pattern of the acoustic transducer (Betteridge *et al*, 2007). In this way, a three frequency ABS will thus have three system constants, with one system constant for each of its component transducers. Whilst an ABS system constant is specific to a given ABS-transducer assemblage, it is independent of the concentration and size of the suspended particle populations the ABS is used to probe. By measuring the backscattered signal from suspensions of particles with known backscattering characteristics (such as glass spheres), over a number of different concentrations and sizes, ABS system constants can be determined and their size and concentration independency confirmed. In addition, comparison of system constants obtained before and after field deployments enables any calibration change during the deployment period to be discerned.

In order to replace a number of aging systems, a new generation of three frequency ABSs was developed and constructed at the Proudman Oceanographic Laboratory (POL) over the period 2003 – 2005, and are hitherto referred to as ABS-1, 2 and 3. To date, these ABSs have mainly been deployed in the Dee estuary experiments and at Sea Palling during LEACOAST2. ABS-2 failed during its first deployment at Sea Palling (March 2006), due

to leakage of its O-ring seals, and was subsequently replaced by a commercial 4 frequency AQUAscat ABS (AQUAtec Group Ltd.) in the next (October 2006) deployment. During recovery of the AQUAscat (January 2007), two of its cable connectors were damaged, and the instrument was returned to the manufacturer for repair and upgrade to twisted pair cables. In addition, also due to a damaged connector, the original 4 MHz transducer for ABS-1 (serial number 110) was replaced with the 4 MHz transducer from the failed ABS-2 (serial number 111), immediately prior to the October 2006 LEACOAST2 deployment.

This report provides a chronological record of the calibrations of ABS-1, ABS-3, and the AQUAscat, carried out at POL over the period 2005 – 2007. Whilst this report does not aim to re-iterate either the experimental or calculation procedures detailed in Betteridge *et al* (2007), certain aspects of these procedures are elaborated upon here to ensure a complete record of the calibrations is achieved.

2 Measurement procedure

All measurements of ABS system constants were made with the ABS transducers submerged in a suspension of borosilicate glass spheres (Ballotini), generated in a sediment tower constructed from a Perspex cylinder 2.15 m high, with a 0.3 m inner diameter and a wall thickness of 1cm (see Figure 1). The sediment tower was filled with 20 μm filtered mains water (~ 133 l) to which 0.2 – 0.4 l of thin domestic bleach were added, to suppress biological growth. The presence of biological cells in the sediment tower could present a number of problems, including flocculation of the glass spheres and additional absorption or scattering of the acoustic signal. The introduction of thin bleach is not expected to significantly affect the speed of sound in the sediment tower. With a density of ~105 % that of water, the relative quantity of bleach added to the sediment tower (up to 0.4 l in 133 l) however, would result in a 0.05 % increase in the density of the dilution mixture.

A rotating propeller/mesh grid assemblage was used to mix the suspension in the lower half of the sediment tower (at ~ 1.2 m depth), and operated at a constant rotation rate throughout all measurements. The rotation rate of the propeller/mesh grid assemblage was set to obtain as near a homogenous suspension of Ballotini in the sediment tower as was possible. Two bilge pumps were attached to the bottom of the sediment tower via a sink hole, and were used to pump the mixed suspension back to the top of the sediment tower, where it was re-introduced via a series of inlets evenly spaced around the circumference of

the sediment tower. The backscattered signal recorded by the ABSs was range-gated into 128, 1cm bins. Whilst the rotation axle itself did not backscatter the sound, a join in the rotation axle (located at ~ 0.85 m depth) along with the mixing assemblage caused enhanced acoustic backscatter from these locations, and therefore measurements of ABS system constants were limited to the top 0.8 m of the sediment tower. All ABSs were set to a pulse repetition frequency of 4 Hz, with an in-hardware ensemble average produced every 32 Hz, generating 1 recorded profile every 8 seconds.

System constants were determined for each transducer of each ABS using three different ¼ φ sieved size fractions of glass spheres, having nominal radii of 115.5, 137.5 and 163.75 μm, with several different concentrations used for each sphere size. Clear water ABS measurements were collected prior to introducing each size of glass sphere into the sediment tower, to measure the background signal. A small background signal was expected due to a combination of instrument noise and any residual suspended particles. Background measurements were recorded for a period of one hour, after which the first concentration of the first size was introduced into the sediment tower, and the ABS allowed to record for a further hour. Pumped water samples of known volume (5 l) were then collected from a number of different heights within the sediment tower, and each water sample passed through a 20 μm aperture filter. The Ballotini trapped during filtering was dried and weighed to determine the mass concentration within the sediment tower, to enable the vertical homogeneity of the suspension to be determined. The second concentration was then introduced and the process repeated. After ABS measurements at all concentrations had been collected, the first size of Ballotini was removed from suspension by means of a 20 μm aperture filtration net placed beneath the inlets at the top of the sediment tower, and left to collect all Ballotini over a period of 1 to 2 days. Background readings were then collected again, and the second Ballotini size introduced, and the process repeated.

Throughout all measurements, care was taken to eliminate the presence of air bubbles in the sediment tower, from both the transducers, and the rotation axle of the propeller/mesh grid assemblage. This was achieved by first letting the sediment tower de-gas before measurements commenced, by operating the bilge pumps intermittently for 15 minute intervals over a period of 3 – 4 days. In addition, all Ballotini added to the sediment tower were wetted and degassed before being introduced. On occasion, small quantities of

(acoustically transparent) washing up liquid were smeared on to the transducers, to lower surface tension and prevent the formation of bubbles. Usually, this was not necessary, though time constraints between successive instrument deployments restricted the amount of time the sediment tower could be left to de-gas where multiple refills were required.

3 Data processing

3.1 Pre-processing of ABS data

Each POL ABS utilised an 8-bit Analogue-to-Digital Converter (ADC), and thus had 256 increments available over which to record backscattered signals. To enable greater distinction between weak signals, the receiver circuit for each measuring frequency included a logarithmic amplifier, thus increasing the dynamic range of the POL ABSs. In order to retrieve meaningful values from the ABS ADC values, the relationship between the receiver circuit input voltage (α_{RC}, in dB relative to 106 mV) and the recorded ADC values was determined in the laboratory, for each measuring frequency of each ABS (see Figure 2). The relationships were observed to follow a linear trend above the noise floor, and a summary of the regression statistics describing each relationship is provided in Table 1. Hence, ABS recorded ADC values were converted into the receiver circuit input voltage (relative to the 106 mV reference) by application of the appropriate relationship polynomials (Table 1) and were subsequently linearised, to retrieve the (dimensionless) ratio of received (V_R) to emitted (V_0) signal:

$$V = \frac{V_R}{V_0} = 10^{(\alpha_{RC}(dB)/20)} \tag{1}$$

In contrast, the AQUAscat ABS employed a 16-bit ADC, and thus had 65,536 increments available over which to record backscattered signals. Due to its large intrinsic dynamic range, the AQUAscat did not employ a logarithmic (or time varying) signal amplifier, and the recorded ADC values were linearly scaled to the received pressure (Stephen Caine, AQUAtec Group Ltd, personnel communication). Consequently, the AQUAscat ABS data did not require any pre-processing.

3.2 Calculation of ABS system constants

Background levels were temporally averaged over the recording period ($\overline{V_B}$), and the temporal average subtracted from the backscattered profiles recorded with the Ballotini in suspension (V_S), to obtain the background corrected backscattered Ballotini signal. The corrected backscattered Ballotini signal was then squared, temporally averaged over the Ballotini recording period, and square rooted, to produce the root mean square Ballotini signal (V_{RMS}) for each concentration and size, in each spatial bin. Algebraically:

$$V_{RMS} = \left(\overline{(V_S - \overline{V_B})^2} \right)^{1/2} \tag{2}$$

Thus, the ABS system constant for each recording frequency, K_t, was calculated following Betteridge *et al* (2007) as:

$$K_t = \frac{V_{RMS} r \psi}{K_S M(r)^{1/2}} e^{2r\alpha(r)} \tag{3a}$$

where

$$K_S = \frac{f}{\sqrt{\rho_S a_0}}, \tag{3b}$$

$$\alpha(r) = \alpha_W + \alpha_S, \tag{3c}$$

with

$$\alpha_S(r) = \frac{3}{4\rho_S r} \int_0^r \frac{\chi M(r)}{a_0} dr \tag{3d}$$

where r was the range from the transducer, M was the mass concentration of Ballotini in suspension at r, a_0 was the nominal Ballotini radius, ρ_S is the density of the Ballotini (stated to be 2548.4 kgm^{-3} by the manufacturer), α_W the attenuation by water (=2.6×10^{-14}×[frequency]^2), α_S the attenuation by the sediments (Ballotini), Ψ accounted for the departure from spherical spreading in the transducer near-field, and the frequency dependency has been omitted for clarity.

The form function, f, and the normalised total scattering cross section, χ, were taken from Betteridge *et al* (2007) to be:

$$f(x) = \frac{(1 - 0.5e^{-((x-1.5)/0.5)^2})(1 + 0.4e^{-((x-1.5)/3.0)^2})(1 - 0.5e^{-((x-5.9)/0.7)^2})x^2}{1.17 + 0.95x^2} \quad (4)$$

and

$$\chi(x) = \frac{0.24(1 - 0.4e^{-((x-5.5)/2.5)^2})x^4}{0.7 + 0.3x + 2.1x^2 - 0.7x^3 + 0.3x^4} \quad (5)$$

In order to calculate the wavelength of sound in water for each transducer, and its corresponding x value for each Ballotini size used, the speed of sound in water was taken to equal 1480 ms^{-1}.

To calculate the sediment attenuation, pump sampled concentration profiles were used to determine the average relationship between sediment tower depth and Ballotini concentration for each size of Ballotini used, via regression (Section 4.1). The resulting regression coefficients were then used to predict Ballotini concentration in each ABS bin, thus enabling the evaluation of the integral in Equation 3d (with χ calculated using Equation 5).

The near-field correction (Ψ) was evaluated for each bin following Downing *et al* (1995), and hence the physical radiating aperture (a_t) of each transducer was required. For the AQUAscat, a_t was supplied by AQUAtec. For the POL ABSs, a_t was determined for each transducer by comparing the measured beam pattern (as supplied by the manufacturer) to the theoretical beam pattern using (Medwin and Clay (1998):

$$Dt = 2J_1(z)/z \quad (6)$$

where Dt was the pressure directivity (beam pattern), J_1 is the first order Bessel function, $z = ka_t\sin\theta$, with k the wavenumber ($=2\pi/\lambda$), θ the angle to the normal from the transducer face, and a_t was incremented from 1 to 20 mm in 0.1 mm intervals. The value of a_t in this range for which the RMS difference between the modelled and measured beam pattern was a minimum, was taken as the physical radiating aperture of each transducer. For the 2 and 4 MHz transducers, measured and modelled beam patterns were compared over θ ranging from 0° to 5°. This range was used owing to larger uncertainties in the measured beam patterns beyond the specified range. For the 1 MHz transducers, comparison was made

over θ ranging from -5° to +5°, due to the presence of noticeable asymmetry in the 1 MHz measured beam patterns. The radiating apertures for each transducer and each ABS are presented in Table 2, along with the transmit and receive sensitivities. A comparison of the measured beam patterns of each transducer, as supplied by the manufacturer, with the beam pattern modelled according to Equation 6 is provided in Figure 3.

4 Results and Discussion

4.1 Homogeneity of the sediment tower

The individual concentration profiles derived from the pumped water samples collected after each Ballotini recording period are presented in Figure 4. Figure 4 shows that pump sampled concentrations increased with depth, indicating the presence of some vertical inhomogeneity within the sediment tower. Whilst the degree of inhomogeneity was within the variability between repeated samples at some depths (i.e. see Figure 4 (a)), the concentration gradient was consistently present for the vast majority of profiles, suggesting it could not be removed by simple temporal averaging of multiple measurements at the sample depths. Figure 4 also shows the measured concentrations were substantially lower in the pump sampled region then their theoretical values. Hence, in order to account for the Ballotini missing from the region sampled, it is likely that concentrations in the un-sampled lower half of the sediment tower continued to increase with depth.

Figure 5 presents the same concentration profiles expressed as relative concentration (concentration divided by the profile mean), and shows that whilst a concentration gradient was consistently present for all Ballotini sizes, it was essentially small, with the greatest departure from the mean being ~ 20 %. Moreover, the concentration gradients were highly linear in the region sampled, and Table 3 presents a summary of the statistics describing linear regressions of relative concentration on sediment tower depth across all profiles collected for each size of Ballotini. The regression coefficients in Table 3 suggest that at the 95 % confidence interval, little difference existed between the concentration gradients in the sediment tower, regardless of Ballotini size. Due to the consistency and high degree of linearity of the concentration gradients in the sediment tower (Figure 5), the average concentration gradients for each Ballotini size were thus used to calculate Ballotini concentration in all bins for each respective calibration run. The predicted Ballotini concentrations were subsequently used to evaluate the sediment attenuation in all bins

using Equation 3d (see Section 3.2). Figure 6 presents a comparison between measured Ballotini concentrations and those predicted using the regression coefficients presented in Table 3, for all pump samples collected. Figure 6 shows predicted Ballotini concentrations were in excellent agreement with measured concentrations, with all predicted concentrations closely scattered around the theoretical 1:1 line. The slope and intercept of a linear regression between predicted and measured Ballotini concentration were 0.984 ± 0.011 and 0.009 ± 0.008 (n = 105, R^2 = 98.7 %), which were not significantly different to 1 and 0 respectively at the 95 % confidence interval. The RMS difference between predicted and measured Ballotini concentrations was 0.04 gl^{-1}.

4.2 POL ABS system constants

All profiles of ABS system constants (K_t) showed a sharp increase from near-zero values in the first 0.1 m from the transducer, caused by cross-talk between the transmitter and receiver during transmission (Betteridge *et al*, 2007). Data from the first 0.2 m of all profiles was therefore excluded from further analysis, to ensure this feature did not contaminate profile averages.

4.2.1 ABS-1

As the original 4 MHz transducer of ABS-1 was replaced in October 2006 (see Section 1), ABS-1 system constants are compared for calibrations conducted before and after this date. Figures 7 and 8 present the K_t profiles obtained from ABS-1 before and after October 2006 respectively, calculated following Equation 3. For the 1 and 2 MHz transducers of ABS-1, K_t was relatively constant at ranges between 0.2 – 0.8 m, as expected, and no significant difference was observed in the magnitude of the mean system constant obtained before and after October 2006. For the 4 MHz transducers, K_t was relatively constant at ranges between 0.2 – 0.4 m, though markedly decayed with increasing range thereafter.

This behaviour was observed for both of the 4 MHz transducers used, though the exact mechanism causing the 4 MHz roll-off remains unclear to date. It was considered that the cause of the 4 MHz roll-off could have been due to the higher total attenuation ($\alpha_W + \alpha_S$) present at this operating frequency. High attenuation could theoretically cause the backscattered Ballotini signal (V_S) to become comparable to the backscattered background signal (V_B) at increased range, which could cause V_{RMS} to tend to zero. This was checked

for ABS-1 in the range 0.2 – 0.8 m, and Figure 9 presents the temporal mean V_S and V_B for each of the calibration runs presented in Figure 7 (i.e. each calibration run obtained pre-October 2006). Figure 9 shows that in the range 0.2 – 0.8 m, the backscattered Ballotini signal was significantly higher then the backscattered background signal for all pre-October 2006 calibration runs, and therefore the 4 MHz roll-off was not attributable to attenuation of the backscattered Ballotini signal.

The profile mean values of K_t for each ABS-1 calibration run are tabulated in Table 4. The depth ranges over which the profile mean K_t values were calculated are provided in Table 5. Although the 4 MHz system constant for ABS-1 increased by ~ 27.5 % following replacement of transducer s/n 110 with transducer s/n 111, the ABS-1 depth mean K_t values showed no significant drift with time for all frequencies (Table 4). Figure 10 presents the variation of the profile mean values of K_t with Ballotini radius and profile mean concentration, for each operating frequency of ABS-1. Figure 10 confirms that the K_t values obtained for ABS-1 were independent of particle size and concentration.

4.2.2 ABS-3

Figure 11 presents the K_t profiles obtained from all calibration runs of ABS-3. As for ABS-1, the K_t profiles obtained for the 1 and 2 MHz transducers were relatively constant at ranges between 0.2 – 0.8 m, with the 4 MHz K_t profiles showing a similar roll-off above ~ 0.4 m. The presence of the 4 MHz roll-off in both ABS-1 and ABS-3 K_t profiles suggests that the cause is common to both systems, rather than damage or malfunction of either system.

The profile mean values of K_t for all ABS-3 calibration runs are tabulated in Table 6 (with the depth ranges over which the profile mean K_t values were calculated provided in Table 5). As, for ABS-1, the depth mean K_t values obtained for ABS-3 also showed no significant calibration drift with time. The variation of profile mean K_t values with Ballotini radius and profile mean concentration are presented in Figure 12 for ABS-3, which confirms that ABS-3 system constants were also independent of particle size and concentration.

The overall mean ABS-3 K_t values showed less variation with frequency then was evident for ABS-1. This was due to differences in the electronics, radiating apertures, and the transmit and receive sensitivities of the two instruments.

4.3 AQUAscat ABS system constants

As the transducer cables and connectors were replaced on the AQUAscat post recovery from the final deployment phase of LEACOAST2, AQUAscat ABS system constants are compared for calibrations conducted before and after this modification (April 2007). Figures 13 and 14 present the K_t profiles obtained from the AQUAscat before and after the cable modifications respectively. AQUAscat K_t profiles collected prior to April 2007 showed some variation with range between 0.2 – 0.8 m (Figure 13), with the 1 MHz profiles showing a small increase with range, and the 4 MHz profiles showing a similar roll-off with range to that observed in the 4 MHz profiles from the POL ABS systems. In contrast, post-April 2007, the AQUAscat K_t profiles were almost completely constant with range, at all operating frequencies, with no roll-off in the 4 MHz K_t profiles discernable (Figure 14). This suggests that the mechanism responsible for causing the 4 MHz roll-off was related to the use of co-axial transducer cables and connectors, and AQUAtec reported a 20 dB lower noise floor for the twisted pair cables relative to the coaxial cables (Stephen Caine, AQUAtec Group Ltd, personnel communication). The exact mechanism behind the 4 MHz roll-off remains elusive however, since Figure 9 suggests that at least for the POL ABS systems (which also use coaxial transducer cables and connectors), the magnitude of the noise floor in the 4 MHz channels was not responsible for the 4 MHz roll-off (see Section 4.2.1).

The profile mean values of K_t for the AQUAscat are tabulated in Table 7 (with the depth ranges over which the profile mean K_t values were calculated provided in Table 5). Table 7 (and Figures 13 and 14) show that the AQUAscat system constants changed significantly at all frequencies after the coaxial cables were replaced with twisted pair. Consequently, no post-deployment calibrations exist for the AQUAscat data collected during the final deployment phase of LEACOAST2, and the AQUAscat K_t values obtained before deployment should be applied to the LEACOAST2 AQUAscat dataset.

Figure 15 presents the variation of profile mean K_t values with Ballotini radius and profile mean concentration for each operating frequency of the AQUAscat, and confirms that the AQUAscat system constants were independent of particle size and concentration.

4.4 AQUAscat ABS system constants calculated using V_{MEAN}

Whilst the AQUAscat system constant values presented in Section 4.3 were calculated correctly in the technical sense, when the AQUAscat data obtained during LEACOAST2 was analysed using the same methodology, numerous spikes were generated in the V_{RMS} records which subsequently lead to erroneous ABS estimates of particle concentration. Whilst the cause of the spikes in V_{RMS} is currently unknown, likely causes are either a problem specific to the LEACOAST2 deployments, or a technical problem with the AQUAscat. The spikes were not present in AQUAscat records of V_{MEAN} however, calculated as:

$$V_{MEAN} = \overline{(V_S - \overline{V_B})} \tag{7}$$

where V_S and V_B are as previously defined (see Section 3.2). To enable the most accurate estimates of particle concentration possible from the LEACOAST2 deployments, it was therefore necessary to calculate the AQUAscat system constants using the same methodology as applied to the analysis of the LEACOAST2 dataset, and therefore Figures 16 and 17 present the K_t profiles obtained from the AQUAscat before and after the cable modifications respectively, derived using V_{MEAN}. Figure 16 and 17 show similar variability of AQUAscat K_t values with range to that already described in Section 4.3. The profile mean values of K_t for the AQUAscat, derived using V_{MEAN}, are tabulated in Table 8 (with the depth ranges over which the profile mean K_t values were calculated provided in Table 5). Table 8 (and Figures 16 and 17) shows that when calculated using V_{MEAN}, the system constants typically showed a slight decrease relative to the system constants calculated using V_{RMS}. It should be noted that within 1 standard deviation however, no significant difference existed between the system constants calculated using the two methods.

Figure 18 presents the variation of profile mean K_t values derived using V_{MEAN} with Ballotini radius and profile mean concentration for each operating frequency of the AQUAscat, and confirms that the AQUAscat system constants were also independent of particle size and concentration when derived using V_{MEAN}.

5 Conclusions

- The measurement procedure and experimental setup described in Section 2 facilitates repeatable and accurate profile measurements of ABS system constants.
- In the POL sediment tower, a vertical concentration gradient was consistently observed for all sizes of suspended Ballotini (glass spheres). The concentration gradient was relatively small, highly linear, and showed little variation with either Ballotini concentration or size.
- The consistency and high linearity of Ballotini concentration gradients in the POL sediment tower enabled concentrations to be predicted to within an RMS error of 0.04 gl^{-1}.
- The system constants derived for each ABS were consistent across the respective calibration runs, excluding changes caused by system modifications.
- Profiles of the 4 MHz system constant showed a roll-off with range for all ABSs when using coaxial transducer cables and connectors. The roll-off was not observed for the AQUAscat following replacement of the coaxial cables with twisted pair. Hence, the POL ABS 4 MHz roll-off is likely caused by a system problem, which may also be related to the use of coaxial cables and connectors.

6 Acknowledgements

This work was supported by the European HYDRALABIII project, and NERC UK as part of its small scale sediment process studies. The authors would like to thank Stephen Caine (AQUAtec Group Ltd) for providing information about the AQUAscat.

7 References

Betteridge, K.F.E, Thorne, P.D. and Cooke, R.D., 2007. Calibrating Multi-frequency Acoustic Backscatter Systems for studying near-bed suspended sediment transport processes. Continental Shelf Research, *Accepted*.

Downing, A., Thorne, P.D. and Vincent, C.E., 1995. Backscattering from a suspension in the near field of a piston transducer. *Journal of the Acoustical Society of America*, 97 (3), 1614 – 1620.

Medwin, H. and Clay, C.S., 1998. Fundamentals of Acoustical Oceanography, *Academic Press*, 712 pp.

Thorne, P.D. and Hanes, D.M., 2002. A review of acoustic measurement of small scale sediment processes. *Continental Shelf Research*, 22, 603 – 632.

Thorne, P.D. and Hardcastle, P.J., 1997. Acoustic measurements of suspended sediments in turbulent currents and comparison with *in-situ* samples. *Journal of the Acoustical Society of America*, 101(5), 2603 – 2614.

Thorne, P.D. and Meral, R., 2007. Formulations for the scattering properties of suspended sandy sediments for use in the application of acoustics to sediment transport processes. *Continental Shelf Research*, *Accepted*.

8 Figures

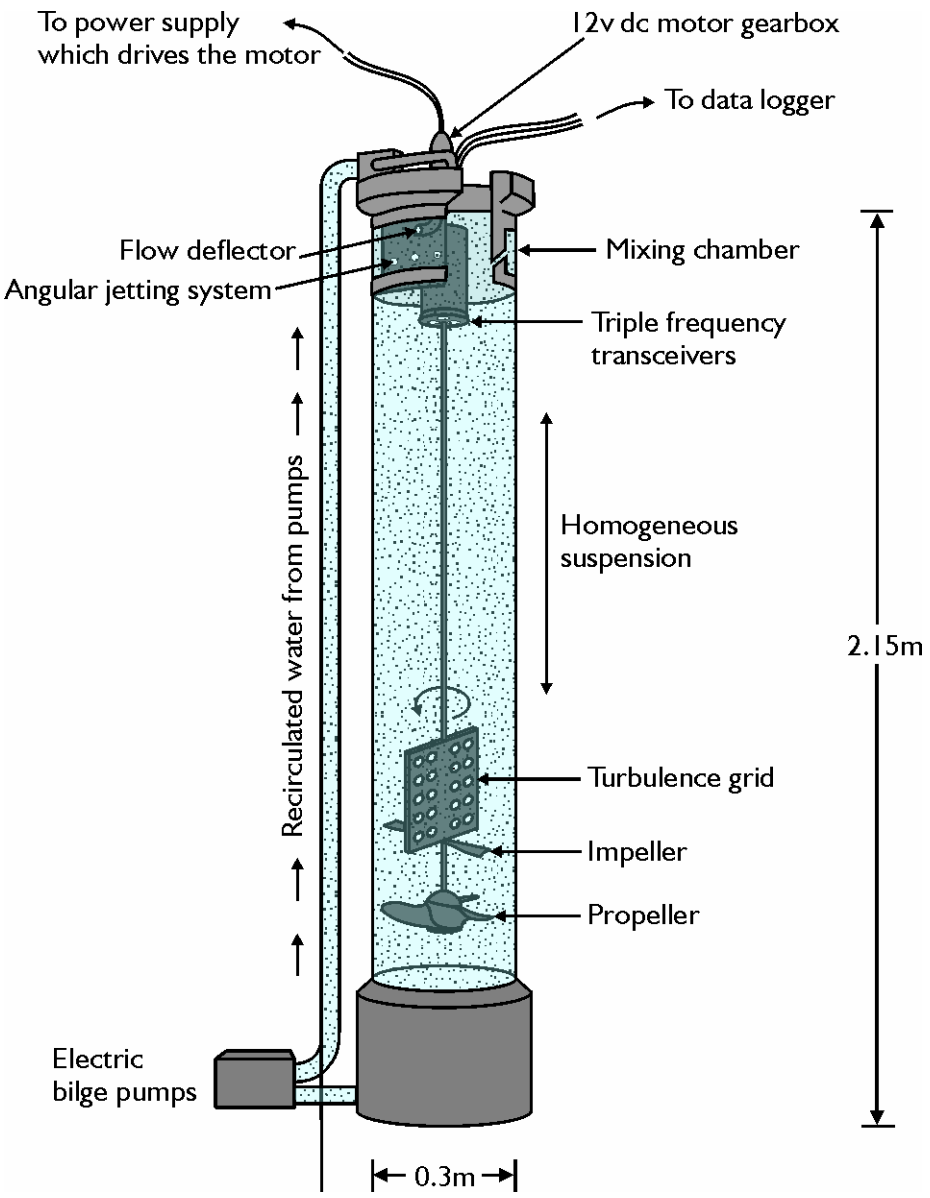

Figure 1 – Conceptual schematic of the POL sediment tower.

(a)

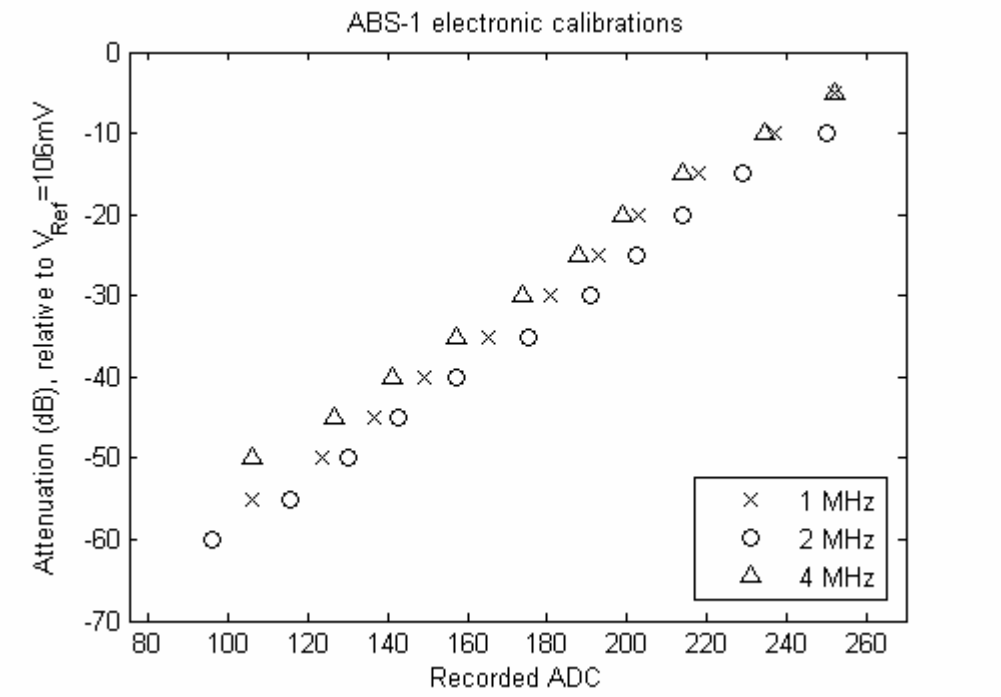

(b)

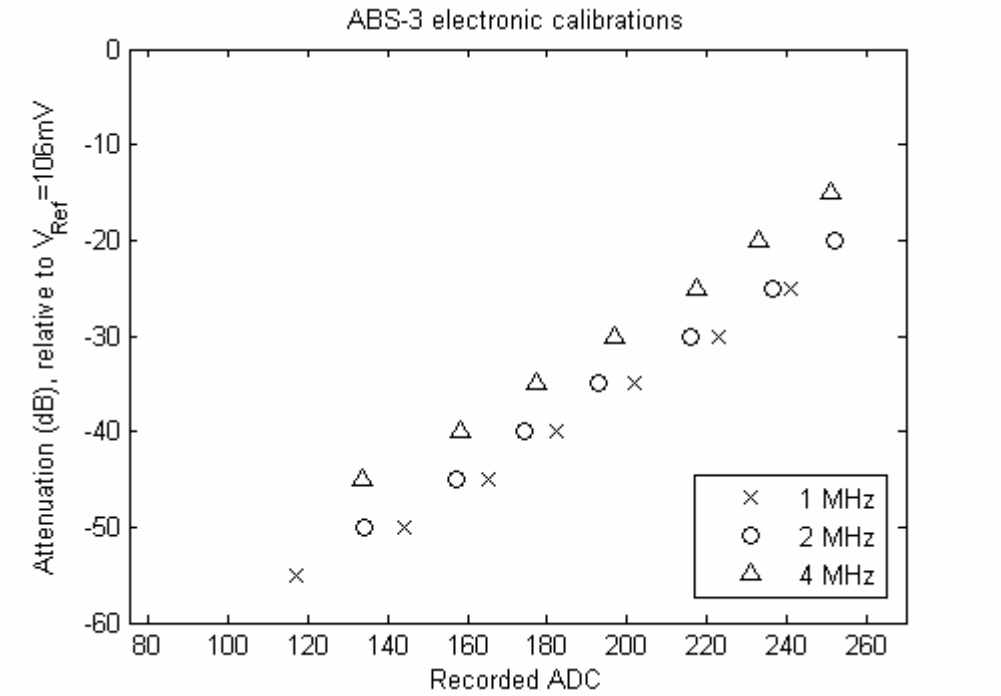

Figure 2 – Laboratory measured variation of recorded ADC values with attenuation (dB), relative to 106 mV, for (a) ABS-1 and (b) ABS-3. Symbols denote the 1 MHz (x), 2 MHz (o) and 4 MHz (Δ) receiver channels for each ABS.

(a)

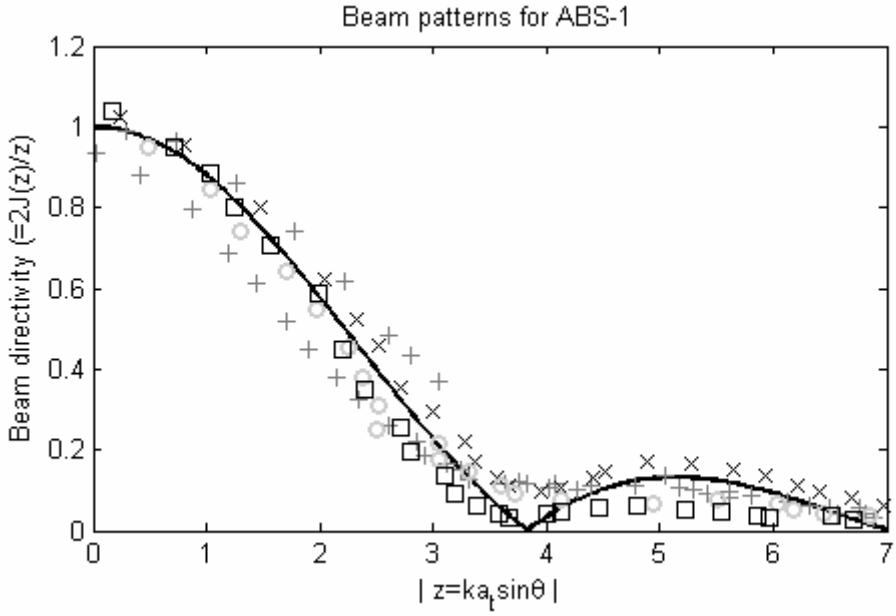

(b)

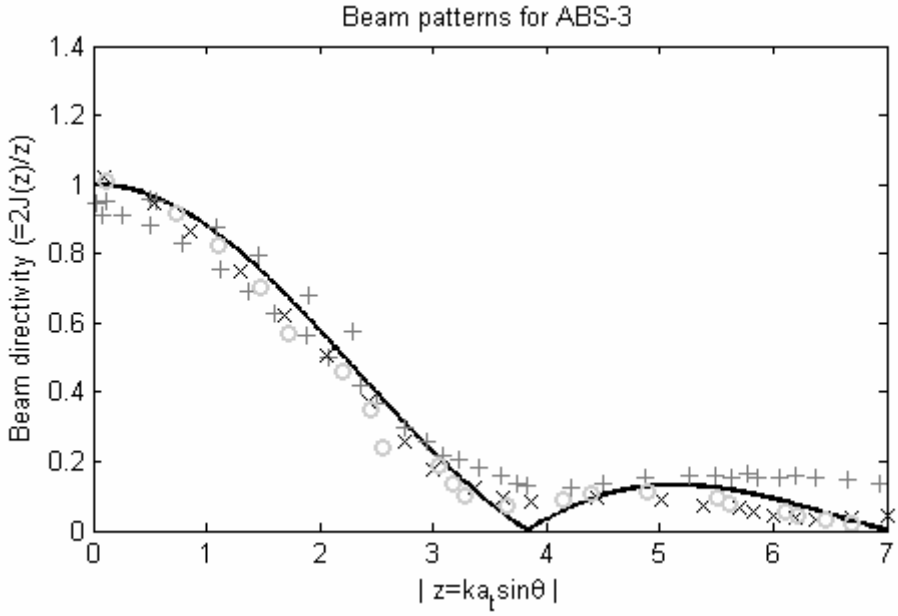

Figure 3 – Comparison of modelled (solid black lines) with measured beam patterns for (a) ABS-1 and (b) ABS-3. Symbols denote the measured beam directivity from the original 1 MHz (+), 2 MHz (x) and 4 MHz (o) transducers for each ABS. Data for the replacement 4 MHz transducer of ABS-1 (serial number 111) are also shown (□) in (a).

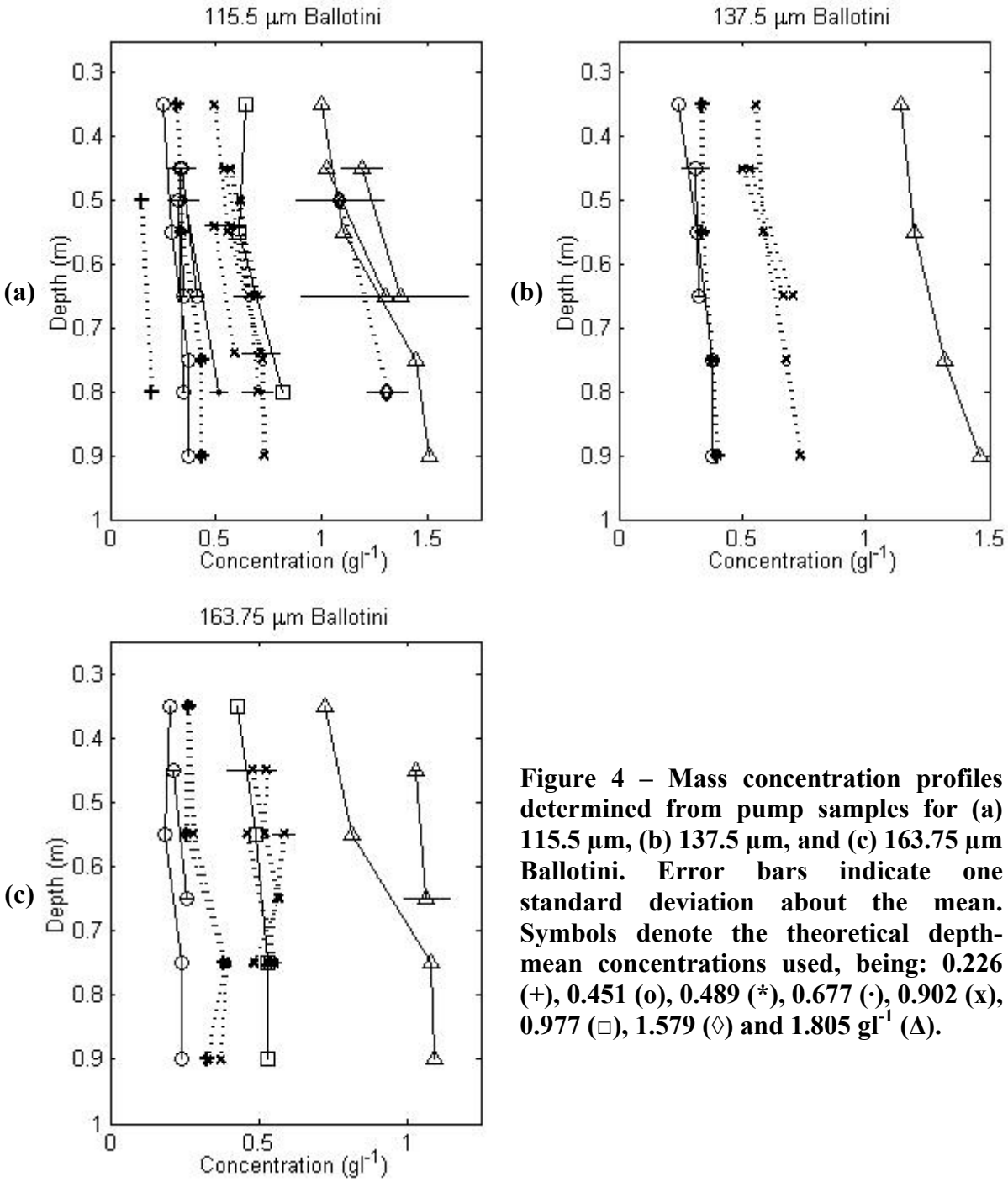

Figure 4 – Mass concentration profiles determined from pump samples for (a) 115.5 µm, (b) 137.5 µm, and (c) 163.75 µm Ballotini. Error bars indicate one standard deviation about the mean. Symbols denote the theoretical depth-mean concentrations used, being: 0.226 (+), 0.451 (o), 0.489 (*), 0.677 (·), 0.902 (x), 0.977 (□), 1.579 (◊) and 1.805 gl^{-1} (Δ).

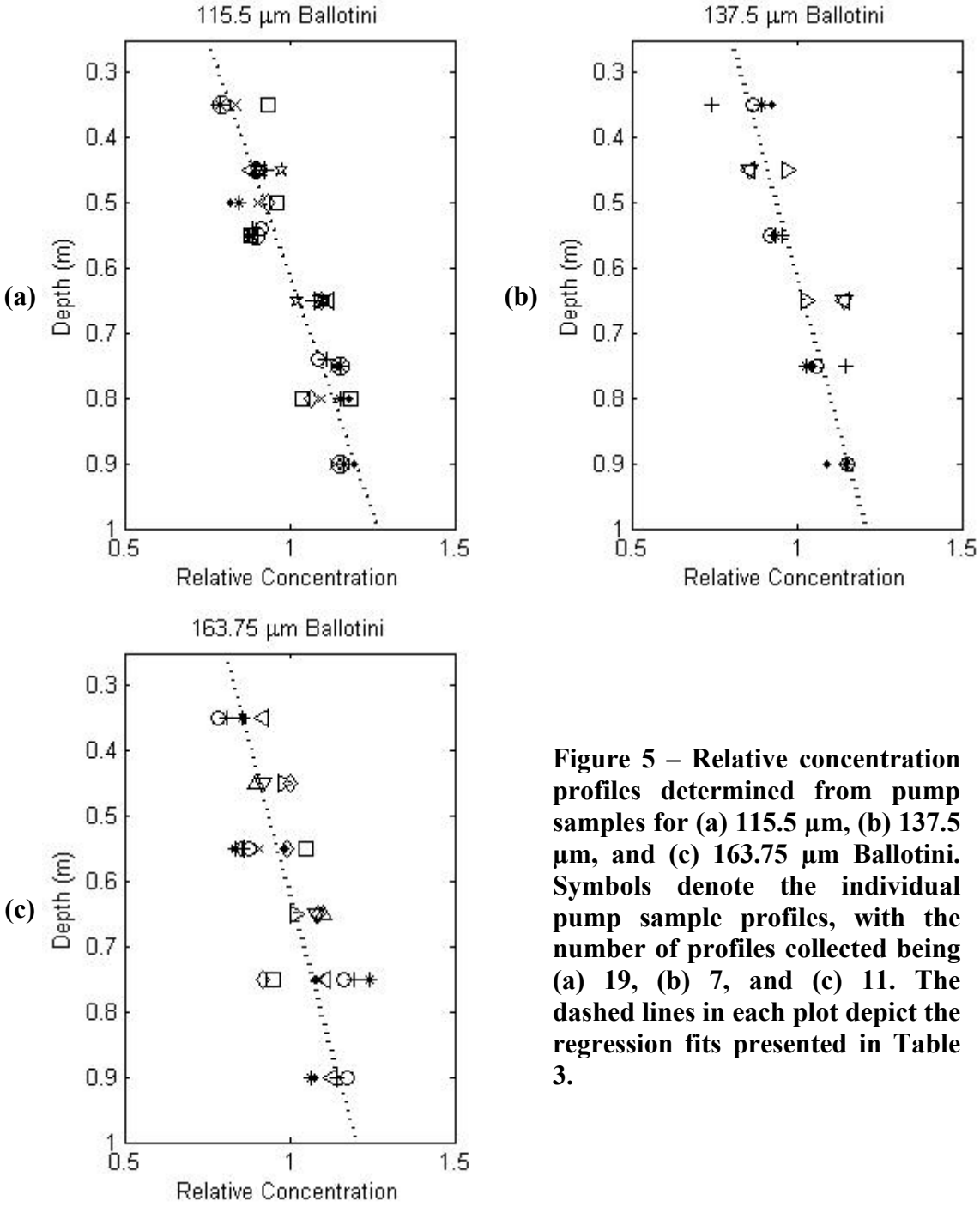

Figure 5 – Relative concentration profiles determined from pump samples for (a) 115.5 µm, (b) 137.5 µm, and (c) 163.75 µm Ballotini. Symbols denote the individual pump sample profiles, with the number of profiles collected being (a) 19, (b) 7, and (c) 11. The dashed lines in each plot depict the regression fits presented in Table 3.

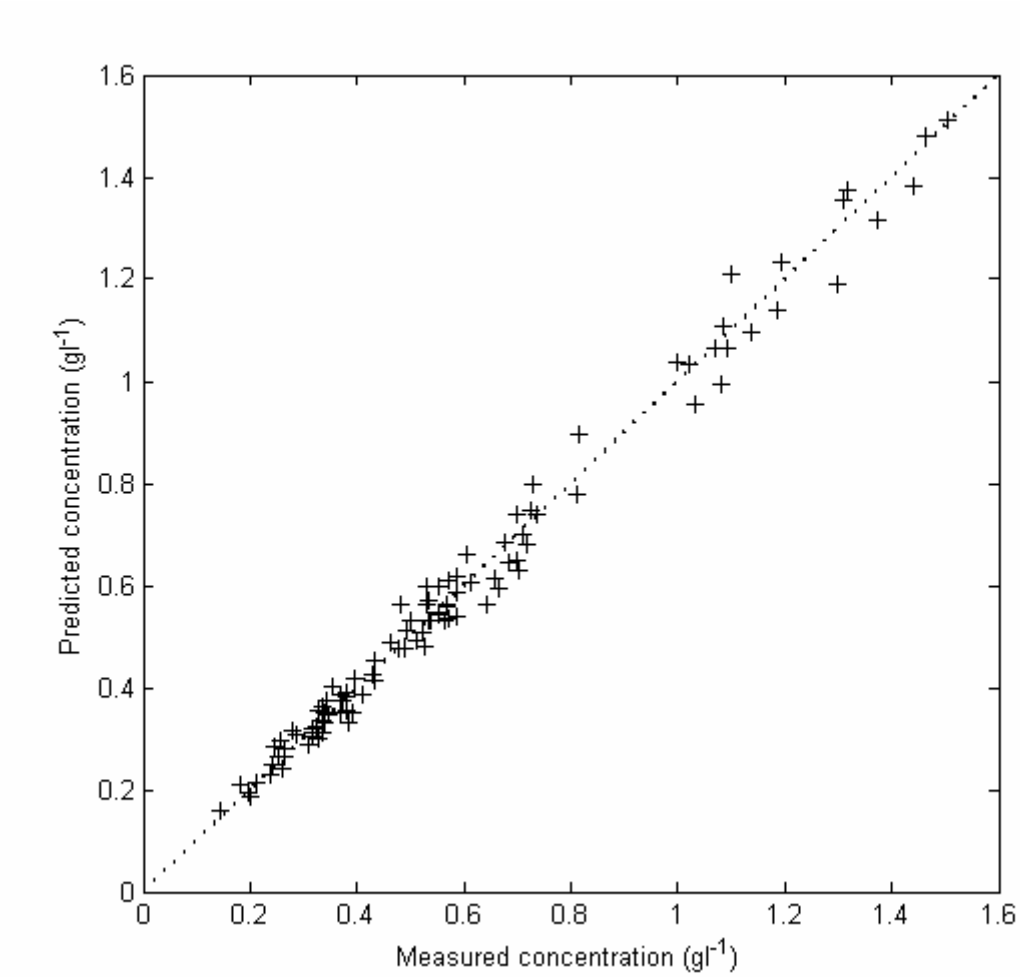

Figure 6 – Comparison between measured and predicted Ballotini concentrations. Predicted concentrations were calculated using the coefficients presented in Table 3. The dashed line depicts the theoretical 1:1 line.

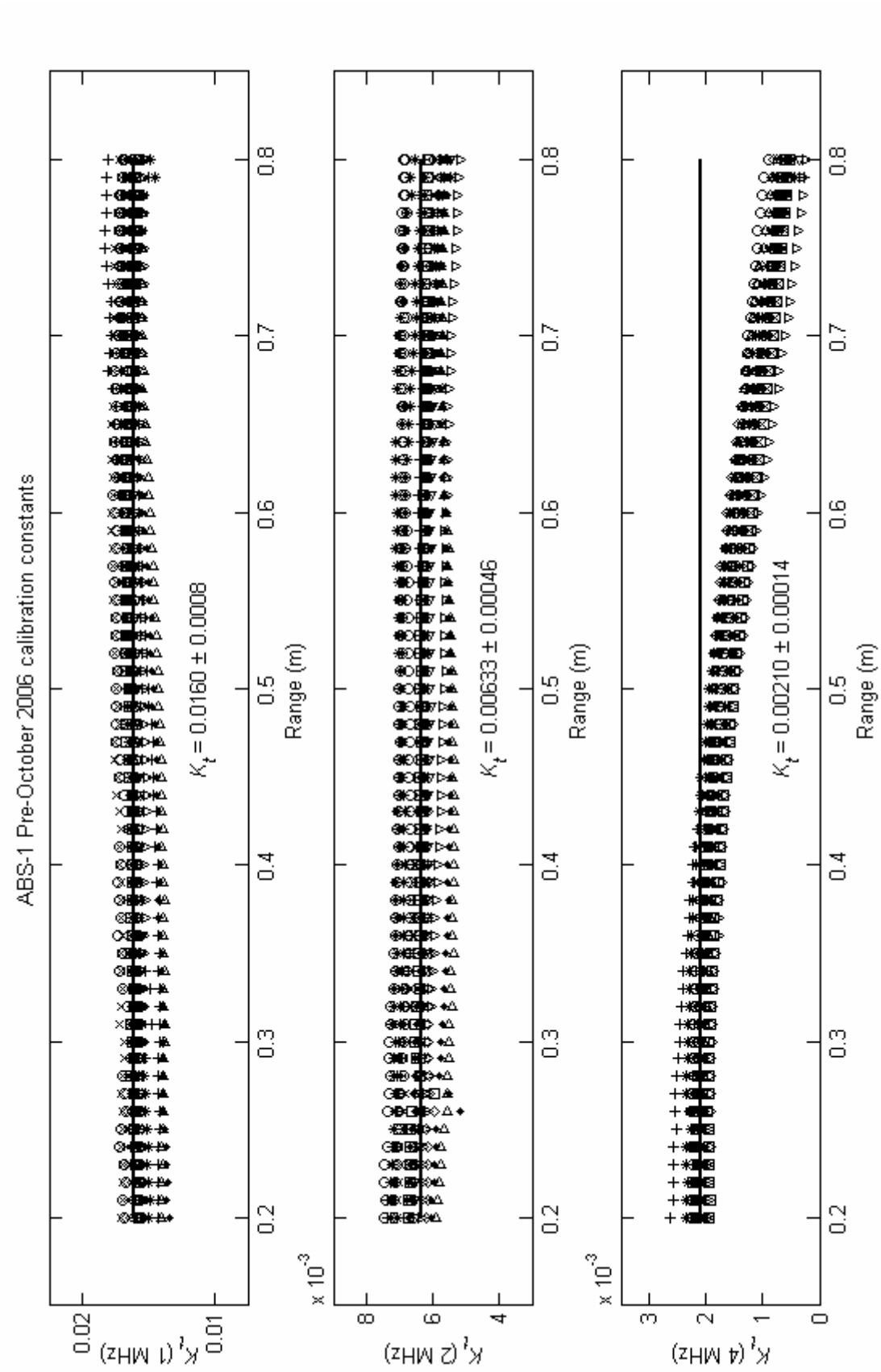

Figure 7 – Variation of ABS-1 K_t with range, for profiles collected pre-October 2006. The different symbols denote individual calibration runs (see Table 4). The solid lines indicate the overall mean K_t for each frequency, listed in each plot.

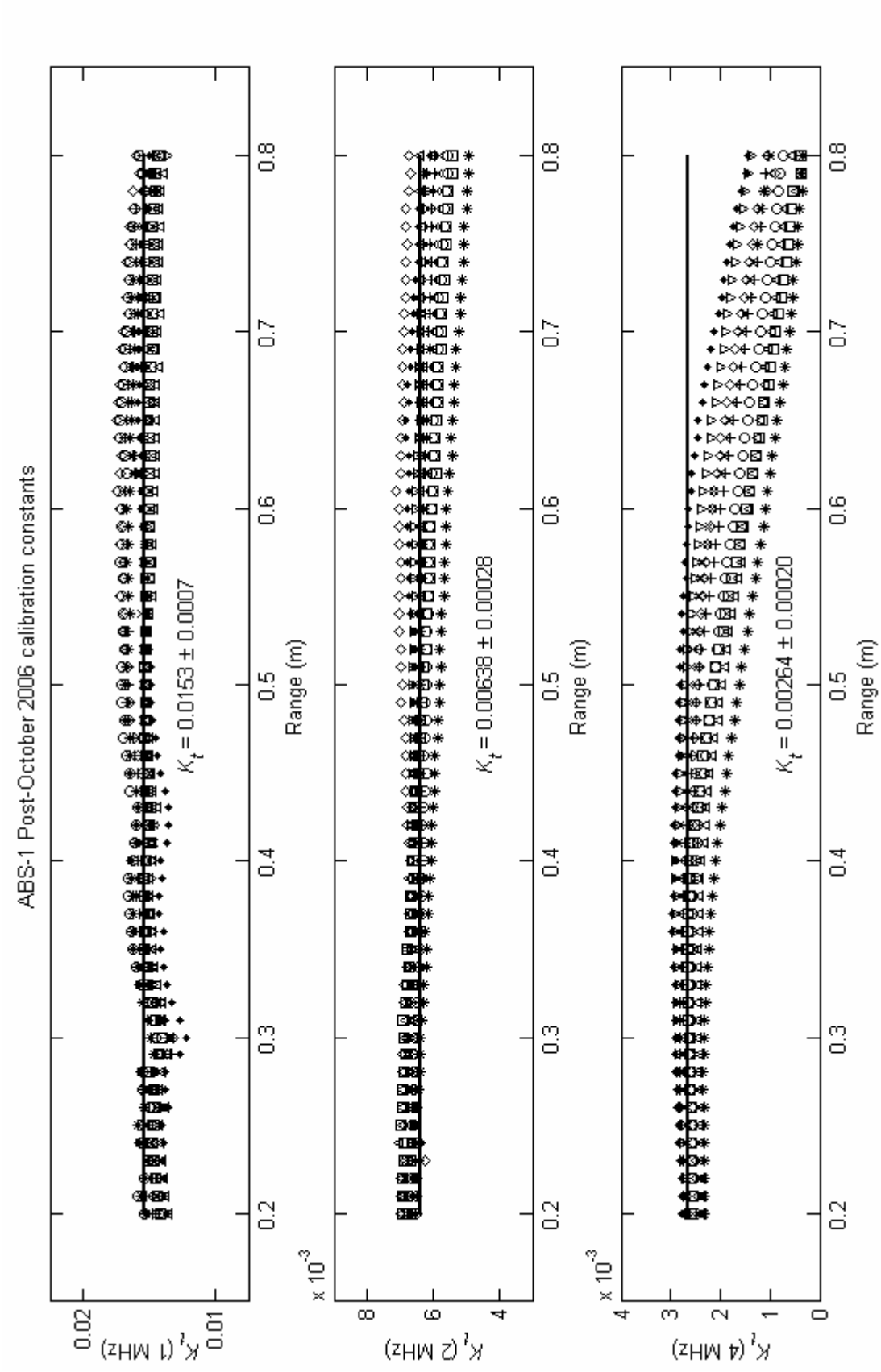

Figure 8 – Variation of ABS-1 K_t with range, for profiles collected post-October 2006. The different symbols denote individual calibration runs (see Table 4). The solid lines indicate the overall mean K_t for each frequency, listed in each plot.

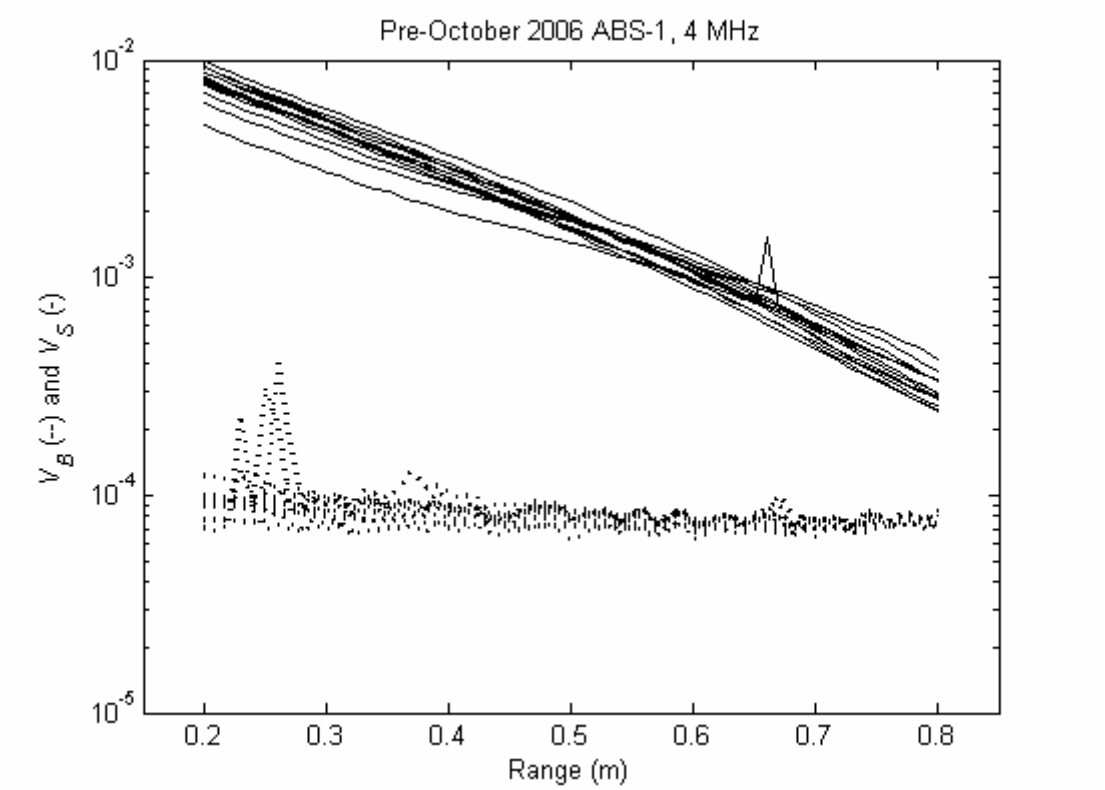

Figure 9 – Comparison of ABS-1 4 MHz backscattered Ballotini signal (V_S, solid lines) and backscattered background signal (V_B, dashed lines) for all pre-October 2006 calibration runs.

(a)

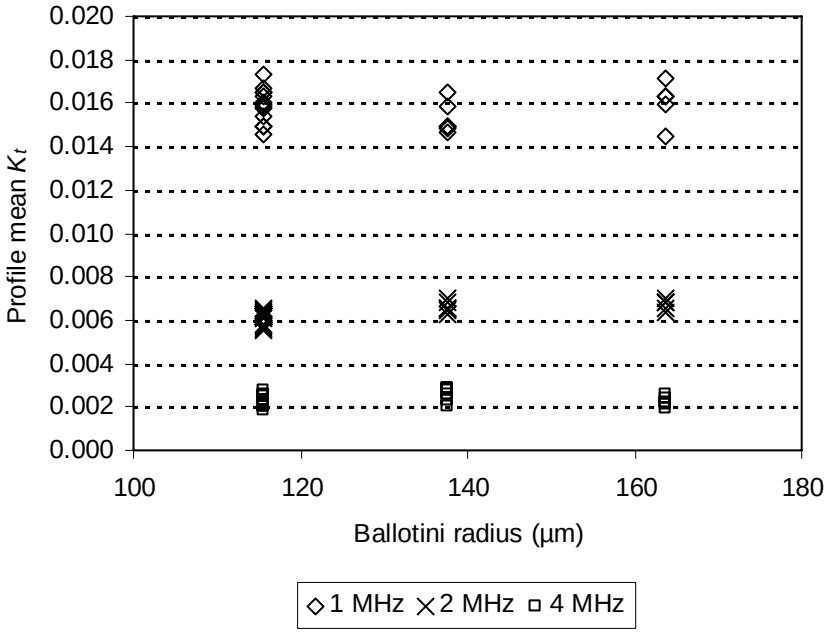

(b)

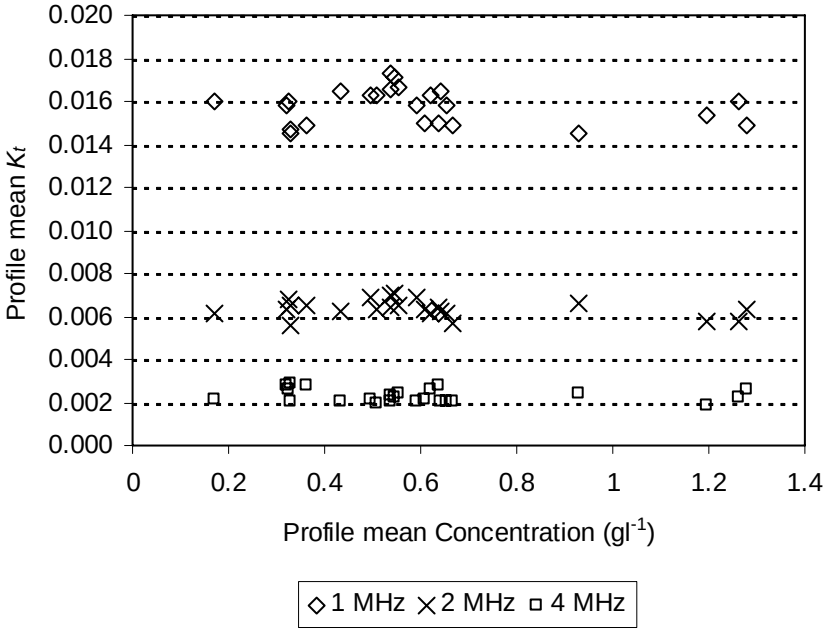

Figure 10 – Variation of all ABS-1 profile mean K_t values with (a) Ballotini radius (µm), and (b) profile mean concentration (gl^{-1}).

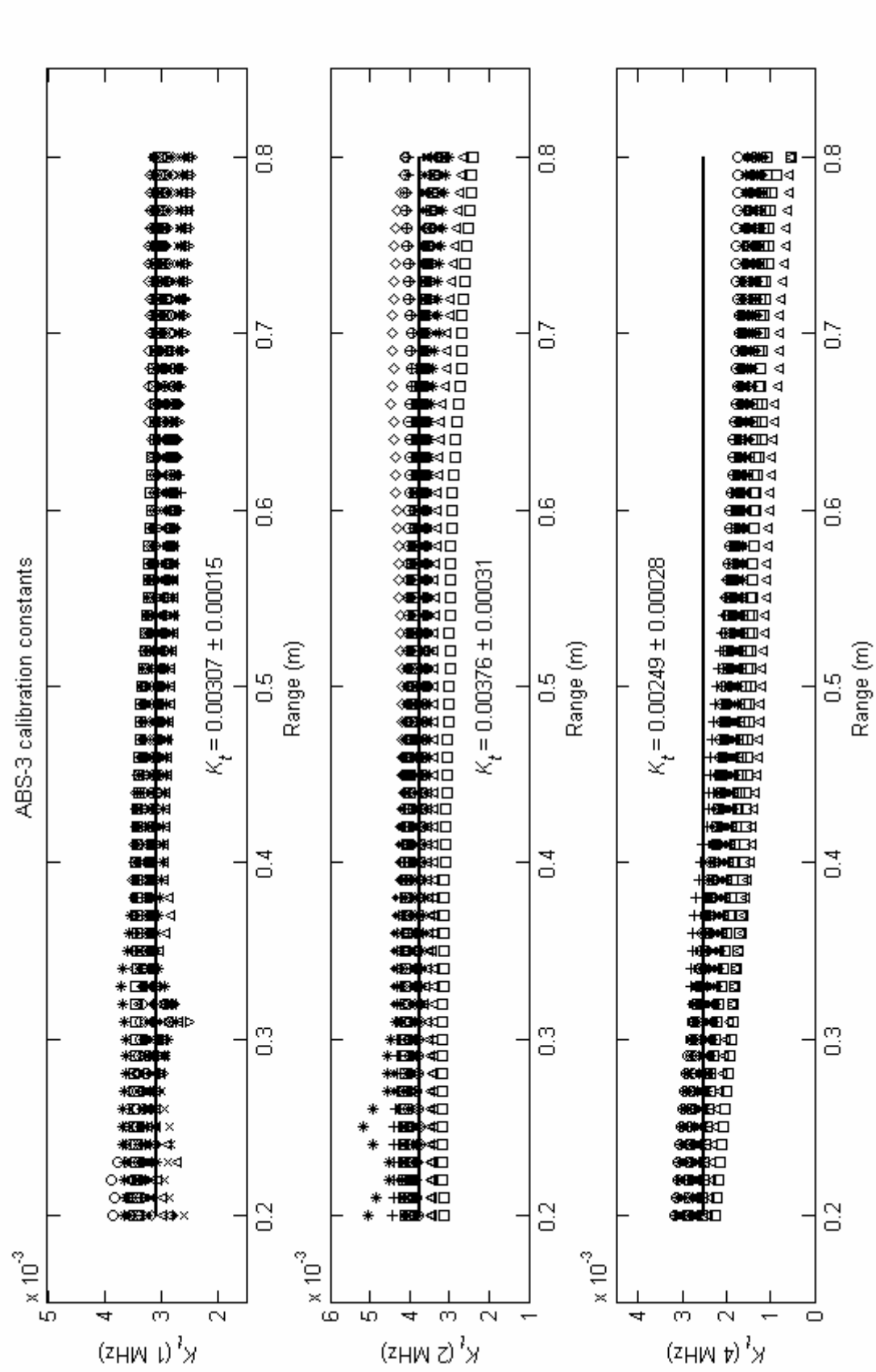

Figure 11 – Variation of ABS-3 K_t with range. The different symbols denote individual calibration runs (see Table 6). The solid lines indicate the overall mean K_t for each frequency, listed in each plot.

(a)

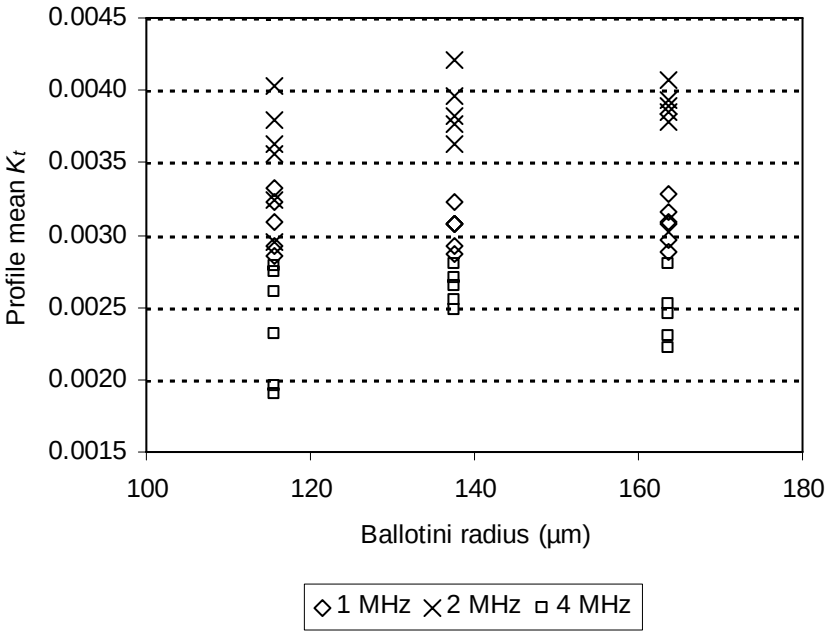

(b)

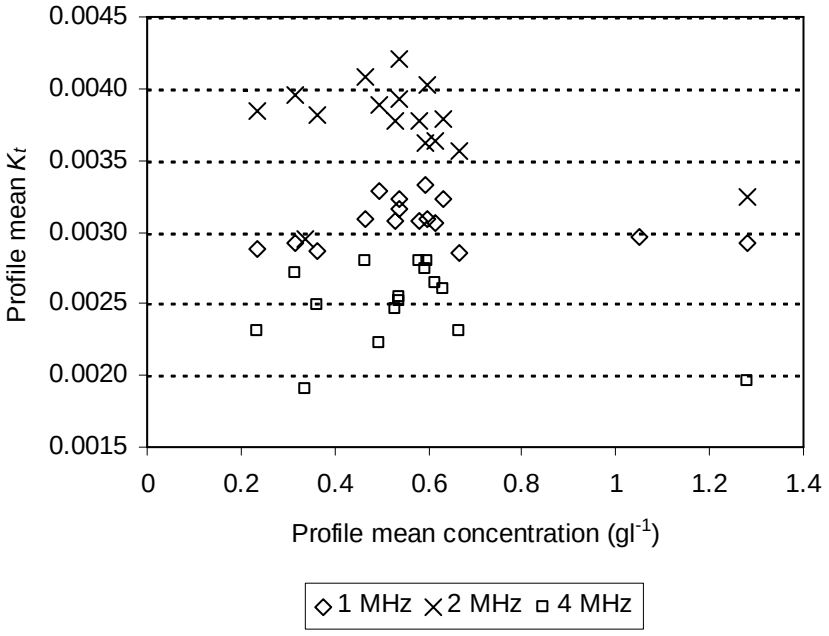

Figure 12 – Variation of all ABS-3 profile mean K_t values with (a) Ballotini radius (µm), and (b) profile mean concentration (gl^{-1}).

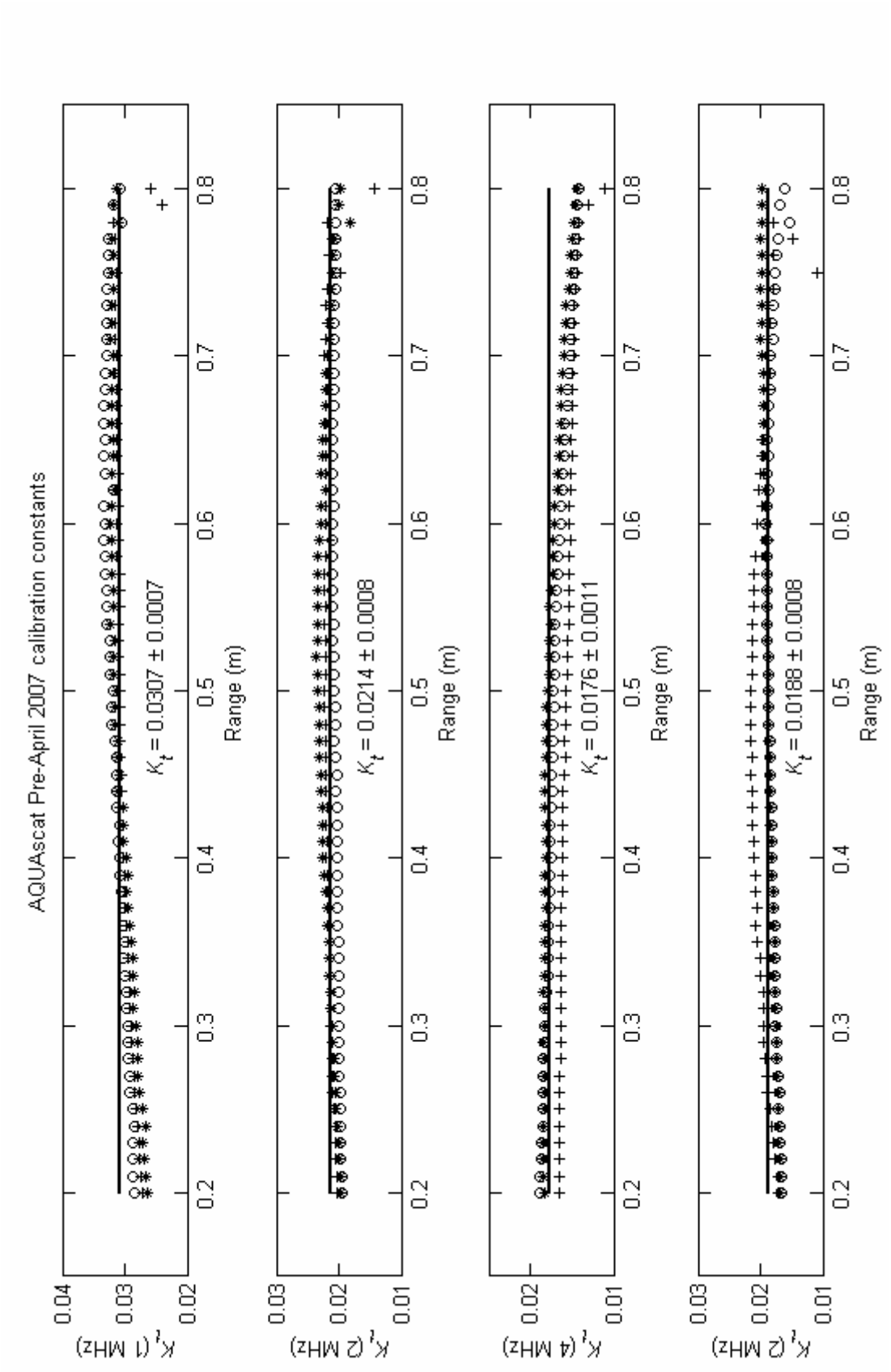

Figure 13 – Variation of AQUAscat K_t with range, for profiles collected pre-April 2007. The different symbols denote individual calibration runs (see Table 7). The solid lines indicate the overall mean K_t for each frequency, listed in each plot.

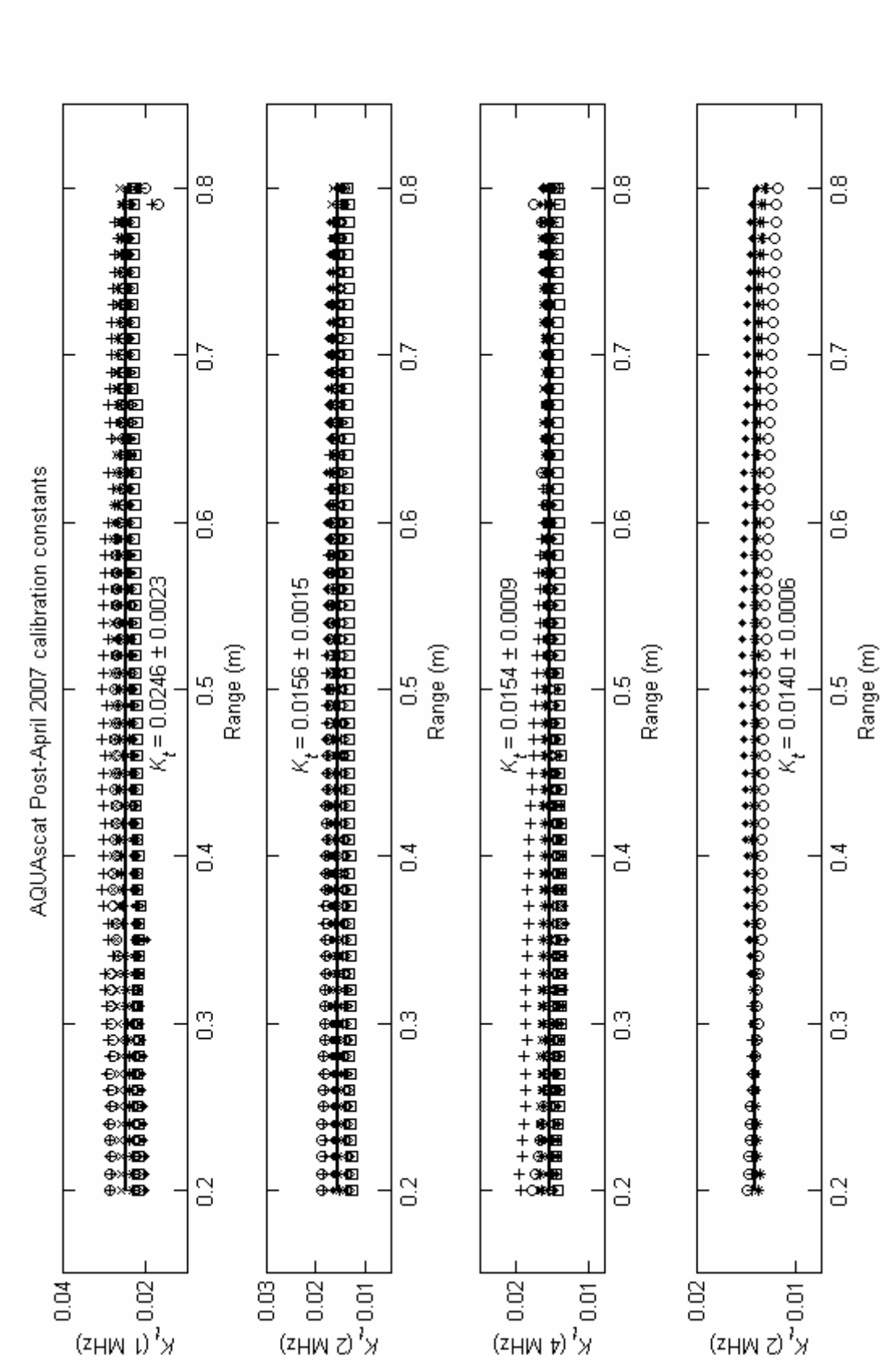

Figure 14 – Variation of AQUAscat K_t with range, for profiles collected post-April 2007. The different symbols denote individual calibration runs (see Table 7). The solid lines indicate the overall mean K_t for each frequency, listed in each plot.

(a)

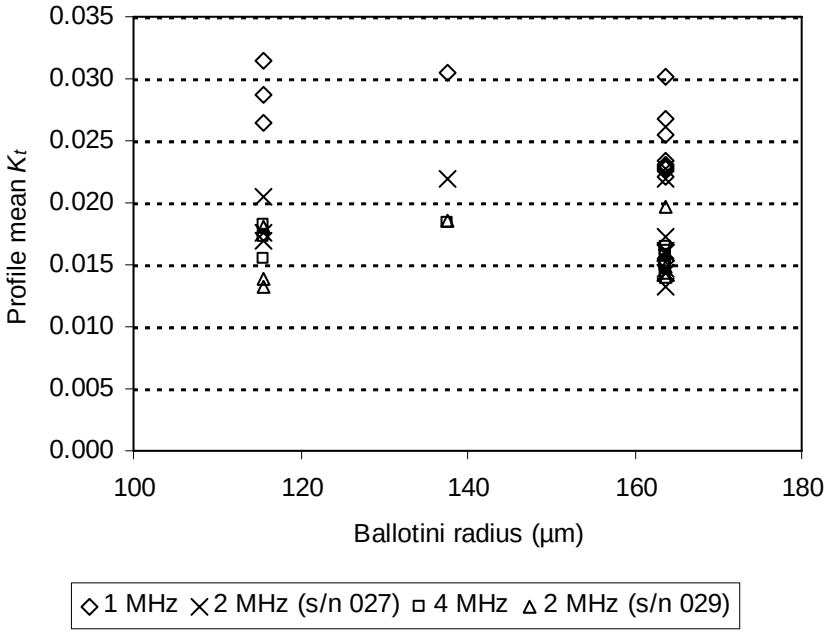

(b)

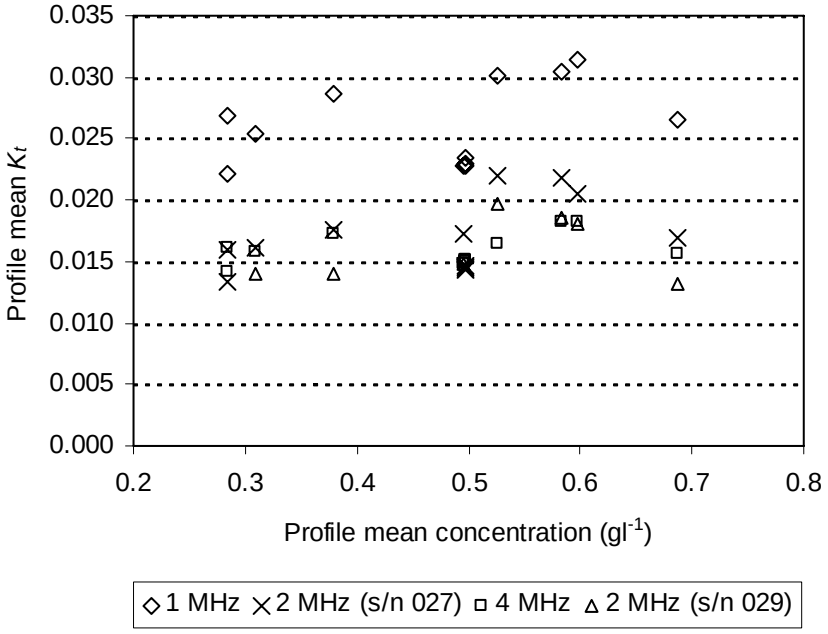

Figure 15 – Variation of all AQUAscat profile mean K_t values, with (a) Ballotini radius (µm), and (b) profile mean concentration (gl^{-1}).

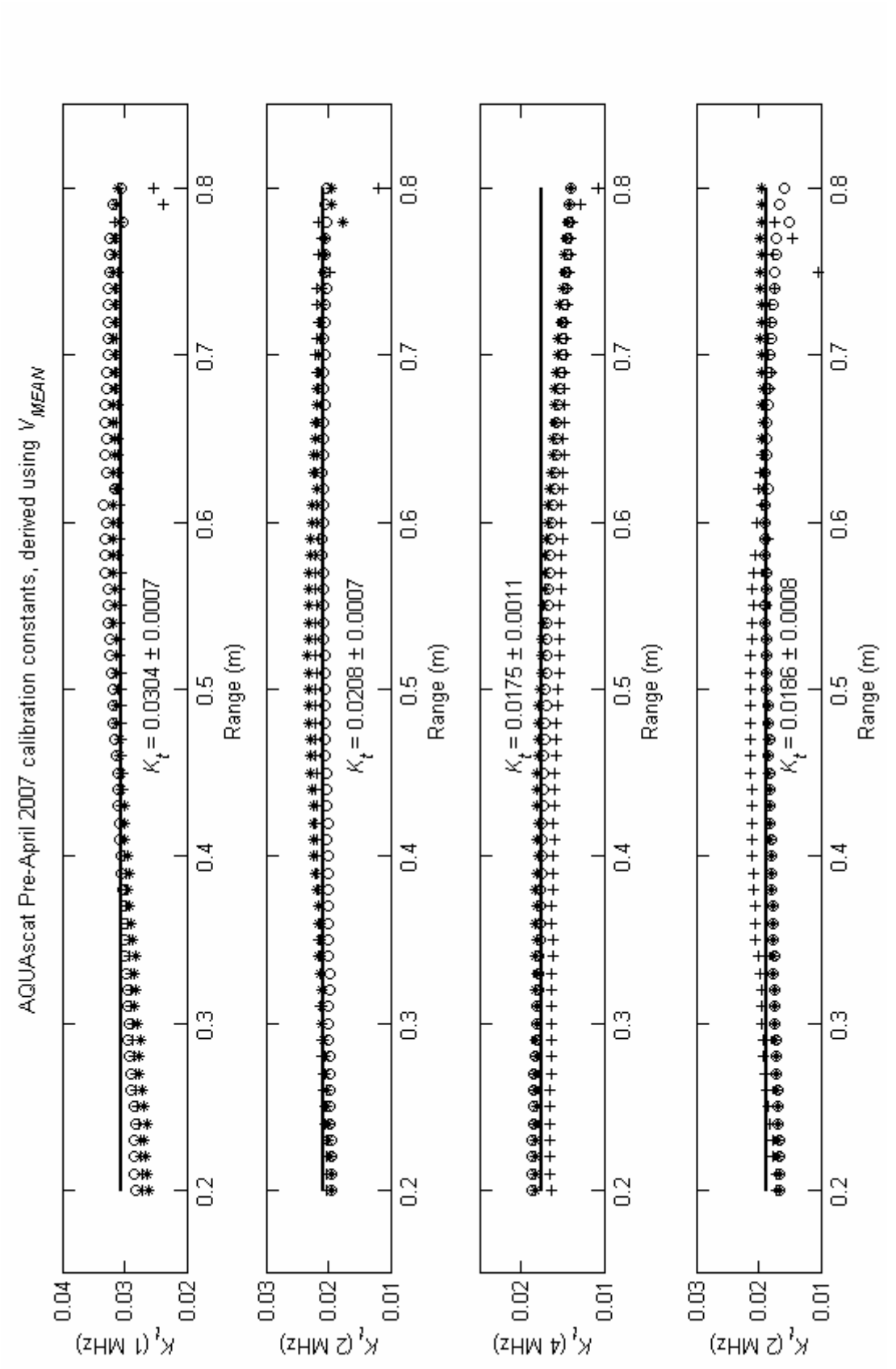

Figure 16 – Variation of AQUAscat K_t with range, obtained using V_{MEAN}, for profiles collected pre-April 2007. The different symbols denote individual calibration runs (see Table 8). The solid lines indicate the overall mean K_t for each frequency, listed in each plot.

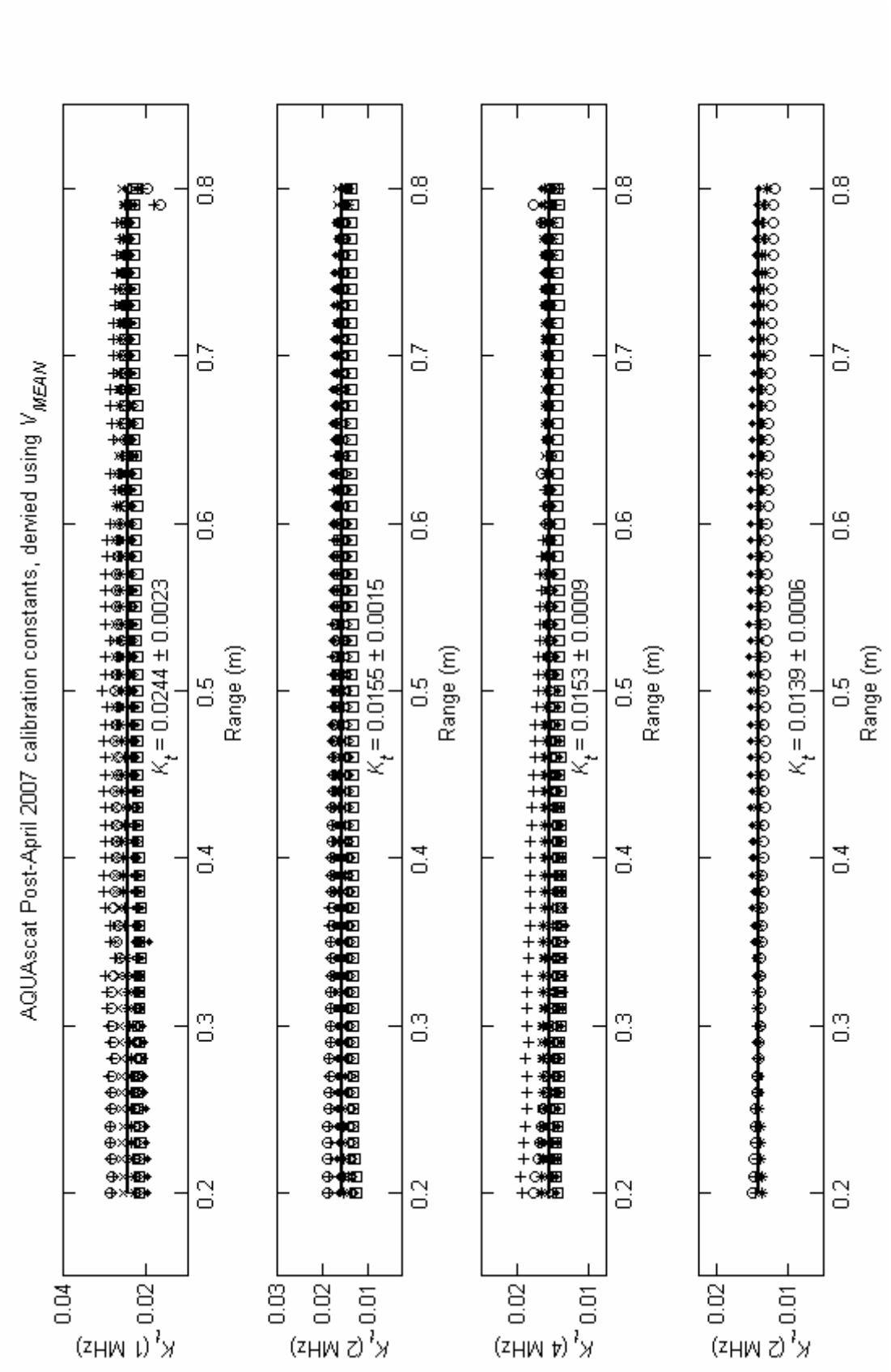

Figure 17 – Variation of AQUAscat K_t with range, obtained using V_{MEAN}, for profiles collected post-April 2007. The different symbols denote individual calibration runs (see Table 8). The solid lines indicate the overall mean K_t for each frequency, listed in each plot.

(a)

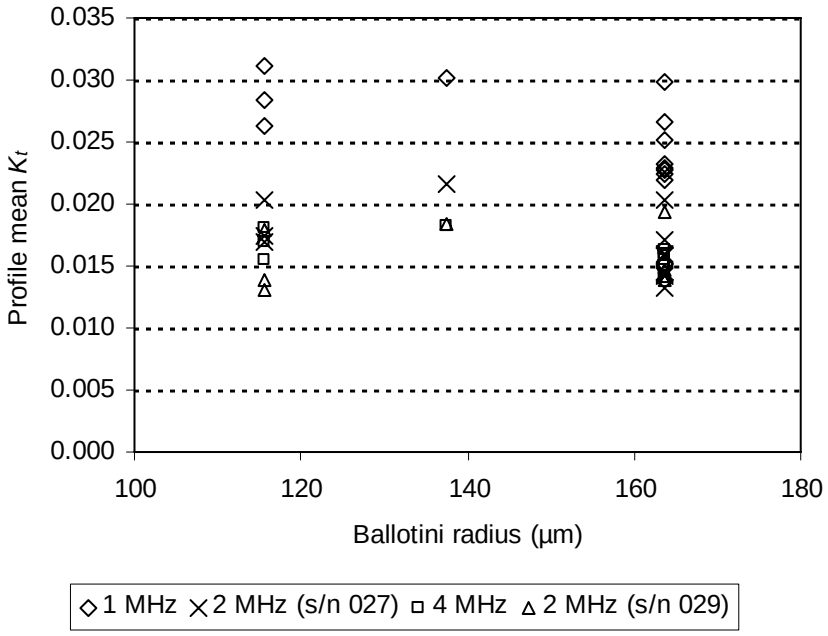

(b)

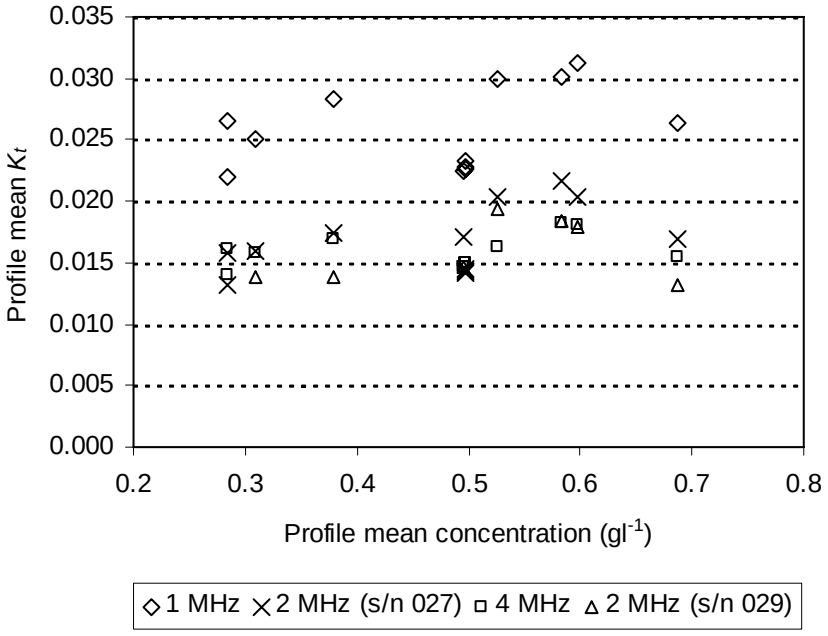

Figure 18 – Variation of all AQUAscat profile mean K_t values, obtained using V_{MEAN}, with (a) Ballotini radius (µm), and (b) profile mean concentration (gl^{-1}).

9 Tables

$\alpha_{RC}\ (dB) = (\alpha \times ADC\ value) + \beta$						
ABS No.	**Frequency (MHz)**	**α**	**β**	**R^2 (%)**	**n**	**Measured**
1	1	0.3509	-92.6662	99.8	11	July 2007
1	2	0.3365	-93.1777	99.7	11	July 2007
1	4	0.3195	-84.7716	99.7	10	July 2007
3	1	0.2457	-84.7642	99.6	7	July 2007
3	2	0.2519	-84.0327	99.6	7	July 2007
3	4	0.2571	-80.2051	99.7	7	July 2007

Table 1 – Regression polynomials relating receiver circuit input voltage (α_{RC}, in dB relative to 106 mV) to ABS recorded Analogue to Digital Converter (ADC) values.

ABS	**Transducer (s/n)**	**F (MHz)**	**a_t (mm)**	**Transmit Sensitivity (dB RE 1µPa/V at 1m)**	**Receive Sensitivity (dB RE 1 V/µPa)**
1	103	1	8.7	179.9	-199.9
1	109	2	6.4	182.6	-208.6
1	110	4	4.9	188.6	-204.9
1	111	4	3.7	189.6	-201.6
3	102	1	6.3	167.0	-203.8
3	108	2	4.1	178.9	-207.5
3	109	4	4.0	188.8	-212.4
AQUAscat	026	1	9.0	Not supplied	Not supplied
AQUAscat	027	2	4.8	Not supplied	Not supplied
AQUAscat	028	4	4.9	Not supplied	Not supplied
AQUAscat	029	2	4.8	Not supplied	Not supplied

Table 2 – Radiating apertures (a_t) and operating frequencies (F), for each transducer of each ABS.

$C_R = (\alpha \times r) + \beta$				
Radius	**α ± Standard Error (S.E.)**	**β ± S.E.**	**R^2 (%)**	**n**
115.5	0.689 ± 0.050	0.580 ± 0.032	80.7	47
137.5	0.545 ± 0.070	0.666 ± 0.045	75.3	22
163.75	0.528 ± 0.079	0.673 ±0.051	58.2	34

Table 3 – Summary of statistics describing regression of relative concentration (C_R) on range (r), for each size of Ballotini.

Date	Operator	Radius (μm)	Conc. (gl^{-1})	K_t (1MHz)	K_t (2MHz)	K_t (4MHz)	Details
24/01/05	KFEB	115.5	0.556	0.0167	0.0065	0.0024	Pre-Dee Experiment '05
26/01/05	KFEB	163.75	0.547	0.0172	0.0070	0.0022	"
18/07/05	KFEB	137.5	0.593	0.0158	0.0069	0.0020	Post-Dee Experiment '05
11/08/05	KL	115.5	0.641	0.0165	0.0062	0.0021	General Calibration
12/08/05	KL	115.5	0.539	0.0173	0.0064	0.0021	"
16/08/05	KL	163.75	0.507	0.0163	0.0063	0.0019	"
31/08/05	KL	115.5	0.171	0.0160	0.0062	0.0021	"
31/08/05	KL	115.5	0.434	0.0165	0.0063	0.0021	"
01/09/05	KL	115.5	1.197	0.0154	0.0057	0.0019	"
05/09/05	KL	115.5	0.331	0.0145	0.0056	0.0020	"
23/09/05	KL	115.5	0.655	0.0158	0.0061	0.0021	"
18/01/06	KFEB	115.5	0.61	0.0150	0.0063	0.0022	Pre-LEACOAST2 Phase-1
26/06/06	KFEB	163.75	0.497	0.0163	0.0068	0.0021	Post-LEACOAST2 Phase-1
27/06/06	KFEB	137.5	0.538	0.0165	0.0070	0.0023	"
28/06/06	KFEB	115.5	0.666	0.0149	0.0056	0.0021	"
Mean (24/01/05 – 28/06/06):				**0.01605**	**0.00633**	**0.00210**	
Standard deviation:				**0.00081**	**0.00046**	**0.00014**	
4 MHz Transducer replaced for s/n 111 October 2006							
15/02/07	BDM	115.5	0.32	0.0158	0.0063	0.0028	Post-LEACOAST2 Phase-2
16/02/07	BDM	115.5	0.622	0.0163	0.0062	0.0026	"
16/02/07	BDM	115.5	1.261	0.0160	0.0058	0.0023	"
20/02/07	BDM	137.5	0.33	0.0147	0.0065	0.0029	"
21/02/07	BDM	137.5	0.638	0.0150	0.0064	0.0028	"
21/02/07	BDM	137.5	1.278	0.0149	0.0063	0.0026	"
28/02/07	BDM	163.75	0.327	0.0160	0.0068	0.0026	"
28/02/07	BDM	163.75	0.929	0.0145	0.0066	0.0024	"
30/04/07	BDM	137.5	0.363	0.0149	0.0065	0.0028	Post-Dee Experiment '07
Mean (15/02/07 – 30/04/07):				**0.01532**	**0.00638**	**0.00264**	
Standard deviation:				**0.00067**	**0.00028**	**0.00020**	
Overall mean:				**0.01577**	**0.00635**	**-**	
Overall standard deviation:				**0.00083**	**0.00040**	**-**	

Table 4 – ABS-1 profile mean K_t values for each calibration run, along with the overall mean and standard deviation. Operator codes are: KFEB: K.F.E. Betteridge, KL: K. Leborde, and BDM: B.D. Moate.

ABS	1 MHz (cm)	2 MHz (cm)	4 MHz (cm)
ABS-1	20 - 80	20 - 80	20 - 40
ABS-3	20 - 80	20 - 80	20 - 40
AQUAscat (Pre-April 2007)	20 – 80	20 – 80	20 - 40
AQUAscat (Post-April 2007)	20 – 80	20 – 80	20 - 80

Table 5 – Depth ranges used to calculate depth mean K_t values for each operating frequency of each ABS.

Date	Operator	Radius (μm)	Conc. (gl^{-1})	K_t (1MHz)	K_t (2MHz)	K_t (4MHz)	Details
21/02/2006	KFEB	163.75	0.464	0.0031	0.0041	0.0028	Pre-LEACOAST2 Phase-1
23/02/2006	KFEB	115.5	0.597	0.0031	0.0040	0.0028	"
22/05/2006	KFEB	115.5	0.595	0.0033	0.0036	0.0027	Post-LEACOAST2 Phase-1
23/05/2006	KFEB	163.75	0.529	0.0031	0.0038	0.0025	"
24/05/2006	KFEB	137.5	0.579	0.0031	0.0038	0.0028	"
26/06/2006	KFEB	163.75	0.497	0.0033	0.0039	0.0022	"
27/06/2006	KFEB	137.5	0.538	0.0032	0.0042	0.0026	"
28/06/2006	KFEB	115.5	0.666	0.0028	0.0036	0.0023	"
02/02/2007	BDM	137.5	0.317	0.0029	0.0040	0.0027	Post-LEACOAST2 Phase-2
02/02/2007	BDM	137.5	0.616	0.0031	0.0036	0.0026	"
08/02/2007	BDM	163.75	0.235	0.0029	0.0039	0.0023	"
09/02/2007	BDM	163.75	0.537	0.0032	0.0039	0.0025	"
09/02/2007	BDM	163.75	1.049	0.0030			"
12/02/2007	BDM	115.5	0.336		0.0029	0.0019	"
13/02/2007	BDM	115.5	0.633	0.0032	0.0038	0.0026	"
13/02/2007	BDM	115.5	1.281	0.0029	0.0032	0.0020	"
30/04/2007	BDM	137.5	0.363	0.0029	0.0038	0.0025	Post-Dee Experiment '07
Overall mean:				**0.00307**	**0.00376**	**0.00249**	
Overall standard deviation:				**0.00015**	**0.00031**	**0.00028**	

Table 6 – ABS-3 profile mean K_t values for each calibration run, along with the overall mean and standard deviation. The missing values on 09/02/2007 (2 and 4 MHz) and 12/02/2007 (1 MHz) were excluded from all analysis due to the presence of bubbles on the respective transducers. Operator codes are as previously defined in Table 4.

Date	Operator	Radius (µm)	Conc. (gl^{-1})	K_t (1MHz)	K_t (2MHz) s/n 027	K_t (4MHz)	K_t (2MHz) s/n 029	Details
30/08/2006	ST	163.75	0.526	0.0301	0.0219	0.0164	0.0196	Pre-LEACOAST2
31/08/2006	ST	115.5	0.598	0.0314	0.0204	0.0182	0.0180	"
26/09/2006	RDCO	137.5	0.583	0.0305	0.0219	0.0183	0.0186	"
Mean (30/08/06 – 26/09/06):				**0.0307**	**0.0214**	**0.0176**	**0.0188**	
Standard deviation:				**0.0007**	**0.0008**	**0.0011**	**0.0008**	
14/05/2007	BDM	115.5	0.379	0.0286	0.0176	0.0172	0.0139	Post-LEACOAST2
14/05/2007	BDM	115.5	0.687	0.0265	0.0170	0.0156	0.0132	"
17/05/2007	BDM	163.75	0.309	0.0254	0.0162	0.0159	0.0140	"
17/05/2007	BDM	163.75	0.496	0.0228	0.0172	0.0148	0.0148	"
18/06/2007	BDM	163.75	0.285	0.0268	0.0160	0.0162	-	-
19/06/2007	BDM	163.75	0.285	0.0221	0.0133	0.0141	-	-
19/06/2007	BDM	163.75	0.497	0.0230	0.0144	0.0151	-	-
19/06/2007	BDM	163.75	0.497	0.0234	0.0146	0.0152	-	-
19/06/2007	BDM	163.75	0.497	0.0228	0.0143	0.0151	-	-
Mean (14/05/07 – 19/06/07):				**0.0246**	**0.0156**	**0.0154**	**0.0140**	
Standard deviation:				**0.0023**	**0.0015**	**0.0009**	**0.0006**	

Table 7 – AQUAscat profile mean K_t values for each calibration run, along with the overall mean and standard deviation before and after the cable modifications. The missing values on 18/06/2007 and 19/06/2007 (2 MHz) are due to the removal of transducer s/n 029 from the AQUAscat on 18/06/2007. Operator codes are as defined in Table 4, with ST: Sarah Taws (AQUAtec), and RDCO: R.D. Cooke.

Date	Operator	Radius (µm)	Conc. (gl^{-1})	K_t (1MHz)	K_t (2MHz) s/n 027	K_t (4MHz)	K_t (2MHz) s/n 029	Details
30/08/2006	ST	163.75	0.526	0.0299	0.0203	0.0163	0.0194	Pre-LEACOAST2
31/08/2006	ST	115.5	0.598	0.0312	0.0203	0.0181	0.0179	"
26/09/2006	RDCO	137.5	0.583	0.0301	0.0216	0.0182	0.0185	"
Mean (30/08/06 – 26/09/06):				**0.0304**	**0.0208**	**0.0175**	**0.0186**	
Standard deviation:				**0.0007**	**0.0007**	**0.0011**	**0.0008**	
14/05/2007	BDM	115.5	0.379	0.0283	0.0175	0.0170	0.0138	Post-LEACOAST2
14/05/2007	BDM	115.5	0.687	0.0263	0.0169	0.0154	0.0131	"
17/05/2007	BDM	163.75	0.309	0.0251	0.0160	0.0158	0.0139	"
17/05/2007	BDM	163.75	0.496	0.0224	0.0171	0.0147	0.0147	"
18/06/2007	BDM	163.75	0.285	0.0266	0.0158	0.0160	-	-
19/06/2007	BDM	163.75	0.285	0.0220	0.0132	0.0140	-	-
19/06/2007	BDM	163.75	0.497	0.0229	0.0143	0.0150	-	-
19/06/2007	BDM	163.75	0.497	0.0233	0.0145	0.0151	-	-
19/06/2007	BDM	163.75	0.497	0.0227	0.0142	0.0150	-	-
Mean (14/05/07 – 19/06/07):				**0.0244**	**0.0155**	**0.0153**	**0.0139**	
Standard deviation:				**0.0023**	**0.0015**	**0.0009**	**0.0006**	

Table 8 – AQUAscat profile mean K_t values for each calibration run, obtained using V_{MEAN}, along with the overall mean and standard deviation before and after the cable modifications. The missing values on 18/06/2007 and 19/06/2007 (2 MHz) are due to the removal of transducer s/n 029 from the AQUAscat on 18/06/2007. Operator codes are as defined in Table 7.